HHS Public Access

Author manuscript

J Endocrinol. Author manuscript; available in PMC 2022 November 24.

Published in final edited form as:

J Endocrinol. ; 252(1): 59–70. doi:10.1530/JOE-21-0298.

Liver is a Primary Source of Insulin-like Growth Factor-1 in Skin Wound Healing

Rita E. Roberts[1,2,4], **Jacqueline Cavalcante-Silva**[1,2,4], **Rhonda D. Kineman**[3,4], **Timothy J. Koh**[1,2,4]

[1]Center for Wound Healing and Tissue Regeneration, University of Illinois at Chicago

[2]Department of Kinesiology and Nutrition, University of Illinois at Chicago

[3]Section of Endocrinology, Diabetes, and Metabolism, Department of Medicine, University of Illinois at Chicago

[4]Research and Development Division, Jesse Brown Veterans Affairs Medical Center, Chicago, Illinois, 60612

Abstract

Insulin-like growth factor (IGF)-1 plays important roles in tissue repair through its ability to stimulate wound cell activity. While IGF-1 is expressed locally by wound cells, liver-derived IGF-1 is also present at high levels in the circulation, and the contributions of local versus circulating IGF-1 to wound levels remain undefined. The hypothesis of this study was that liver is a primary source of IGF-1 during skin wound healing. To test this hypothesis, we utilized a model that allows inducible ablation of IGF-1 specifically in liver of adult mice. We demonstrate that ablation of liver IGF-1 leads to >85% loss of circulating IGF-1 and ~60% decrease in wound IGF-1 during the proliferative phase of healing in both male and female mice. This reduction of liver-derived IGF-1 did not alter local mRNA expression of IGF-1 in wounds. Knockdown of liver IGF-1 significantly delayed wound re-epithelialization, and reduced granulation tissue formation and collagen deposition. Knockdown of liver IGF-1 also significantly reduced angiogenesis and resulted in persistent macrophage accumulation. In summary, liver is a primary source of IGF-1 in skin wounds, and contributes to many aspects of both epithelial and dermal healing.

Introduction

Wound healing requires the coordinated responses of diverse cell types and molecular pathways which participate in overlapping phases of coagulation, inflammation, proliferation and remodeling (Eming, et al. 2014; Singer and Clark 1999). During each

Correspondence: Dr. Timothy J. Koh, University of Illinois at Chicago, Center for Wound Healing and Tissue Regeneration, Department of Kinesiology and Nutrition, 1919 W. Taylor Street, Chicago, IL 60612-7246; Phone number: 312-413-9771; Fax: 312-413-3699; tjkoh@uic.edu.

Author contributions

RR helped design the study, conducted experiments, performed assays and data analysis and wrote the manuscript. JS helped perform assays, data analysis and write the manuscript. RK helped design the study, write the manuscript and provided materials, TK helped design the study, write the manuscript, and provided materials.

Competing interests

All authors have no financial conflicts of interest to report.

stage of healing, endogenous chemokines, cytokines and growth factors play critical roles in regulating proliferation, migration and other functions of inflammatory cells, keratinocytes, fibroblasts, and endothelial cells during the repair process (Martins-Green, et al. 2013; Werner and Grose 2003). In turn, a variety of cell types produce and secrete growth factors during wound healing (Mirza and Koh 2015; Werner and Grose 2003), but the primary source(s) are often uncertain.

Insulin-like growth factor (IGF)-1 plays important roles in wound healing through its ability to stimulate proliferation and migration of keratinocytes, endothelial cells and fibroblasts (Deng, et al. 2012; Haase, et al. 2003; Kanekar, et al. 2000). IGF-1 protein levels are increased in skin wounds compared to normal skin, but wound IGF-1 levels are reduced in diabetic mice and humans (Blakytny and Jude 2006; Brown, et al. 1997; Mirza, et al. 2013). Unlike other growth factors involved in wound healing, IGF-1 is present at high levels in the circulation and the liver is the major source of circulating IGF-1 in mice (Yakar, et al. 1999). In humans, IGF-1 levels in wounds are correlated with those in blood, suggesting that blood is the primary source of wound IGF-1 (Wagner, et al. 2003). However, IGF-1 is also expressed by keratinocytes, fibroblasts and macrophages in skin wounds (Brown et al. 1997; Gartner, et al. 1992; Todorovic, et al. 2008). Thus, the relative contributions of liver IGF-1 and locally produced IGF-1 during wound healing remains unclear.

To determine whether the liver is a primary source of IGF-1 during wound healing we utilized a model of inducible depletion of IGF-1 specifically in the liver of adult mice. Here, we demonstrate that ablation of liver IGF-1 leads to >85% loss of circulating IGF-1 and ~60% decrease in wound IGF-1 during the proliferative phase of healing in both male and female mice. This decrease in IGF-1 results in impaired epithelial and dermal healing, supporting the importance of liver-derived IGF-1 in skin wound healing.

Materials and Methods

Animals.

B6.129(FVB)-Igf1tm1Dlr/J mice were purchased from the Jackson Laboratory (Bar Harbor, ME) and bred at the Jesse Brown VA Medical Center. These mice have loxP sites flanking exon 4 of the *Igf1* gene (IGF-1 fl/fl mice). Mice were housed in environmentally controlled conditions with a 12-hr light/dark cycle. Water and food were available *ad libitum*. Each experiment was performed at least twice with a total of N= 4-8 male and female mice per group/condition. To minimize bias, mice were randomly assigned to experimental groups and resulting samples were coded and analyzed in a blinded fashion. All animal studies were approved by the Animal Care and Use Committee of the Jesse Brown VA Medical Center.

IGF-1 ablation.

To ablate IGF-1 specifically in liver hepatocytes, AAV8.pTBG.Cre (AAV-Cre) was injected via lateral tail vein in IGF-1 fl/fl mice to induce cre-mediated recombination and AAV8.pTBG.Null (AAV-Null) was injected into IGF-1 fl/fl mice for controls (Penn Vector Core, University of Pennsylvania). AAV8-pTBG-Cre mediated recombination has proven to be highly specific for hepatocytes and induces >90% reduction in the expression of the

floxed allele for up to 8 months (Cordoba-Chacon, et al. 2015; Sarmento-Cabral, et al. 2021; Wolf Greenstein, et al. 2017).

Wound model.

Seven days after AAV injection, full thickness excisional skin wounding was performed as previously described (Mirza et al. 2013). Four 8-mm excisional wounds were made on the back of each mouse with a dermal biopsy punch and wounds were covered with Tegaderm (3M). Tegaderm was held in place with a custom made jacket. External wound closure measurements were made using digital images of the dorsum of each mouse recorded immediately after wounding and prior to wound harvest on days 3, 6 and 10 post-injury. Wound area was measured using Fiji Image J and expressed as a percentage of the area immediately after injury. After euthanasia, wounds were collected and either snap frozen in liquid nitrogen for protein or RNA measurements or mounted in tissue freezing medium for histological analysis.

ELISA.

Liver or wound samples were homogenized in cold buffer ice-cold PBS (supplemented with 25 mM β-glycerophosphate, 25 mM NaF, 1 mM Na3VO4, and protease inhibitor cocktail (Sigma); 10 μL per mg liver or wound tissue) using a dounce homogenizer and then centrifuged. Supernatants were used for IGF-1 ELISA as per the manufacturer's instructions (R&D Systems). All samples were run in duplicate and all important comparisons were run on the same plate.

Western blotting.

Homogenates prepared for ELISA were also used for Western blotting. After determining sample protein concentration (Pierce 660 nm Protein Assay Kit, Thermofisher Scientific), aliquots with equal protein were subjected to SDS-PAGE, transferred to nitrocellulose, and total protein on blots measured with Revert 700 Total Protein Stain (#926-11011 LI-COR). Blots were blocked with Intercept Blocking Buffer (#927-60001 LI-COR), incubated overnight with primary antibody (Akt: #9272S, p-Akt: #9271S, p70: #9202S, p-p70: #9205S; Cell Signaling), washed, incubated for 1 hour with secondary antibody (anti-rabbit, #925-32211; LI-COR), washed, and imaged (LI-COR Odyssey CLx). A molecular weight ladder was run with each blot to verify size of intended target. Densitometry of each protein normalized to densitometry of Revert stained blot for that lane (Empiria Studio 1.3 Software, LI-COR).

PCR.

Tissue samples were homogenized using Trizol reagent (#15596018, Thermo Fisher Scientific) and a bead homogenizer. Homogenates were centrifuged and supernatants were used for RNA isolation. RNA concentration was measured using a Nanodrop 2000 (Thermo Fisher Scientific) and equal amounts of RNA were reverse transcribed using the High Capacity cDNA Reverse Transcription Kit (#4368814; Applied Biosystems). mRNA expression was assessed using Power SYBR Green PCR Master Mix (#4367659; Applied Biosystems) and the ViiA7 Real-Time PCR System (Applied Biosystems) by quantitative

PCR (qPCR). mRNA copy number of all transcripts from tissue homogenates were adjusted upon calculation of individual normalization factors with separate GAPDH and RPL-4 housekeeping genes using GeNorm 3.3, as previously described (Vandesompele, et al. 2002). Primers sequences included: GAPDH (F: 5'- ATGGCCTTCCGTGTTCCTAC-3'/ R: 5'- CCTGCTTCACCACCTTCTT), RPL4 (F: 5'-GGATGTTGCGGAAGGCCTTGA-3' / R: 5'-GAGCTGGCAAGGGCAAAATGAG-3') and IGF-1 (F: 5'-ACAGGCTATGGCTCCAGCA-3''/R: 5'-GCACAGTACATCTCCAGTCTCCTC-3').

Wound histology.

Re-epithelialization and granulation tissue thickness were measured in cryosections taken from the center of the wound (found by serial sectioning through the entire wound) and stained with hematoxylin and eosin (Mirza et al. 2013; Mirza, et al. 2014). Digital images were obtained using a Keyence BZ-X710 All-in-One Fluorescence Microscope with a 2x or 20× objective and analyzed using ImageJ. Percentage of re-epithelialization, length of epithelial tongues and granulation tissue area was measured in three sections per wound and was averaged over sections to provide a representative value for each wound.

Angiogenesis was assessed by immunohistochemical staining for CD31 (390, 1:100; Biolegend), macrophage accumulation by staining for F4/80 (BM8, 1:100, eBiosciences) and neutrophil accumulation by staining for Ly6G (1A8, 1:100, BD Pharmingen). Collagen deposition was assessed using Masson trichrome staining (IMEB, San Marcos, CA). For each assay, digital images were obtained covering the wound bed (2–3 fields using a 20× objective) and the percent area stained was quantified by the number of clearly stained pixels above a threshold intensity and normalizing to the total number of pixels. The software allowed the observer to exclude artifacts. For each assay, three sections per wound were analyzed.

Statistics.

Data are expressed as mean ± SD. Statistical significance of differences was evaluated by two-way ANOVA. Sidak's multiple comparison post-hoc test was used to assess differences between groups at each time point. $P < 0.05$ was considered statistically significant.

Results

Liver IGF-1 ablation reduced plasma IGF-1 levels.

To specifically deplete IGF-1 in liver, we administered AAV8 expressing Cre recombinase to IGF-1 fl/fl mice and assessed effects on IGF-1 mRNA and protein in liver and blood over the course of healing. This model of AAV-Cre mediated recombination has proven to be highly specific for hepatocytes (Cordoba-Chacon et al. 2015; Sarmento-Cabral et al. 2021; Wolf Greenstein et al. 2017). Administration of AAV-Cre resulted in near complete ablation of liver IGF-1 mRNA in both male and female mice, both prior to skin wounding and throughout the course of healing, compared to AAV-Null injected controls (Figure 1A). In addition, administration of AAV-Cre reduced protein levels of IGF-1 by >95% in liver and by >85% in peripheral blood plasma prior to wounding in both male and female mice (Figure 1B,C). Following skin wounding, IGF-1 levels in liver and plasma of AAV-Cre

treated mice remained dramatically lower than those in AAV-Null treated mice throughout the course of healing (Figure 1B,C). Ablation of liver IGF-1 did not alter 4 hour fasted blood glucose levels one week after injection of AAV and prior to wounding (197 ± 53 mg/dL for AAV-null mice versus 189 ± 29 mg/dL for AAV-cre mice) or on day 6 after wounding (220 ± 47 mg/dL for AAV-null mice versus 217 ± 2 mg/dL for AAV-cre mice).

Liver IGF-1 knockdown reduced wound IGF-1 levels

We then assessed the effects of liver IGF-1 knockdown on wound IGF-1 protein and mRNA levels. In AAV-Null treated control mice, IGF-1 protein levels increased dramatically on day 3 after wounding and remained elevated through day 10 in both male and female mice (Figure 2A). However, wound IGF-1 accumulation was significantly blunted in AAV-Cre treated compared to AAV-Null treated controls; liver IGF-1 knockdown reduced wound IGF-1 levels by ~60% on days 3 and 6 post-wounding. Importantly, IGF-1 mRNA levels did not differ between AAV-Cre and AAV-Null treated mice, either before or after wounding (Figure 2B). Thus, liver IGF-1 knockdown resulted in decreased wound IGF-1 protein levels without affecting wound IGF-1 mRNA expression.

IGF-1 can activate signaling through a pathway involving Akt and p70. Thus, we assessed levels of total and phosphorylated Akt and p70 by Western blotting (Figure S1). Levels of both total and phosphorylated Akt and p70 increased after wounding in AAV-Null treated mice, as did the ratio of phosphorylated to total levels of each protein (Figure S1), suggesting activation of this pathway during wound healing. However, none of these measurements differed between AAV-Null and AAV-Cre mice. Thus, knockdown of liver IGF-1 did not appear to influence signaling through this pathway.

Liver IGF-1 knockdown delayed wound closure.

Re-epithelialization involves proliferation and migration of keratinocytes and IGF-1 promotes these keratinocyte functions (Emmerson, et al. 2012; Haase et al. 2003; Semenova, et al. 2008). We performed measurements of wound closure in digital images of the wound surface (Figure 3A,B) as well as measurements of re-epithelialization and epithelial tongue lengths in histological sections from the center of the wound (Figure 3 C–E). Measurements of wound closure and epithelial tongue lengths showed progressive increases over the course of healing reaching nearly full closure on day 10 post-injury. In addition to a significant main effect of treatment in analysis by two-way ANOVA, AAV-Cre treated mice showed significantly reduced wound closure, re-epithelialization and epithelial tongue lengths compared to AAV-Null treated controls on day 6 post-wounding (Figure 3A–D). In short, liver IGF-1 knockdown resulted in delayed wound closure.

Liver IGF-1 knockdown impaired granulation tissue formation and maturation

Repair of skin wounds requires dermal healing as well as re-epithelialization, and IGF-1 can promote granulation tissue formation and maturation through its ability to influence fibroblast and endothelial cell activity (Brandt, et al. 2015; Deng et al. 2012; Kanekar et al. 2000; Nakao-Hayashi, et al. 1992). We measured granulation tissue, collagen deposition and angiogenesis in histological sections from the center of the wound. As expected, granulation tissue formation was robust early after wounding in both male and female AAV-Null treated

controls and decreased through the course of healing (Figure 4A,B). In addition to a significant main effect of treatment in analysis by two-way ANOVA, AAV-Cre treated mice exhibited significantly decreased granulation tissue deposition early in the healing process compared to AAV-Null treated controls, with significant differences on day 3 post-wounding and a trend still evident on day 6.

As dermal wound healing progresses, collagen is deposited in the dermis. As expected, collagen deposition assessed by Trichrome staining increased through the course of healing in both male and female AAV-Null treated controls (Figure 4A,C). In addition to a significant main effect of treatment in analysis by two-way ANOVA, AAV-Cre treated mice showed reduced collagen deposition later in the healing process compared to AAV-Null treated controls, with significant differences on days 6 and 10 post-injury in the combined data.

Angiogenesis is a key component of granulation tissue formation, important for delivering oxygen and nutrients to the healing tissue. Angiogenesis showed the expected pattern of formation and regression in AAV-Null treated controls, with CD31 staining peaking on day 6 post-wounding (Figure 5). In addition to a significant main effect of treatment in analysis by two-way ANOVA, AAV-Cre treated mice showed significantly reduced angiogenesis on day 6 in the combined data. In short, liver IGF-1 knockdown impaired dermal healing, by reducing angiogenesis, granulation tissue formation and maturation.

Liver IGF-1 knockdown results in persistent macrophage accumulation.

Inflammation is another key component of wound healing, playing important roles in both dermal and epidermal healing (Koh and DiPietro 2011). We measured macrophage and neutrophil accumulation in histological sections from the center of the wound. Both neutrophils and macrophages showed rapid accumulation in wounds of AAV-Null treated mice, with Ly6G+ and F4/80+ cells peaking on day 6 post-wounding and decreasing by day 10 (Figure 6). Although neutrophil accumulation was not influenced by liver IGF-1 knockdown, macrophage accumulation was significantly higher on days 6 and 10 post-injury in wounds of AAV-Cre treated mice, suggesting that liver IGF-1 may contribute directly or indirectly to the reduction of macrophages during resolution of inflammation in wounds.

Discussion

IGF-1 protein levels increase in skin after injury and play important roles in wound healing; however, the contributions of local versus circulating IGF-1 to wound healing have remained controversial. Since the liver is the primary source of circulating IGF-1, we utilized a model that induces near complete ablation of liver IGF-1 in mice. Here, we demonstrate that ablation of liver IGF-1 in adult mice leads to ~60% decrease in wound IGF-1 levels during the proliferative phase of healing. Knockdown of liver IGF-1 significantly impaired wound re-epithelialization, granulation tissue formation and collagen deposition. Knockdown of liver IGF-1 also significantly reduced angiogenesis and resulted in persistent macrophage accumulation. In short, liver is a primary source of IGF-1 in skin wounds, and liver IGF-1 contributes to both epithelial and dermal healing in mice.

A previous study reported findings on the role of liver IGF-1 in skin wound healing (Botusan, et al. 2018) that appear to conflict to those of the present study. This previous study utilized a mouse model generated by crossing Mx-Cre with floxed IGF-1 mice that enables interferon-inducible knockdown of IGF-1 primarily in liver and leukocytes, resulting in a reduction of ~75% in circulating IGF-1 levels. However, such a reduction did not result in a significant change in external measurements of wound closure, in the histological appearance of granulation tissue, or in CD31 or collagen staining. The differing results compared to the present study may be due to the greater reduction in circulating IGF-1 achieved and more specific targeting of liver IGF-1 in the present study. The AAV8.pTBG.Cre vector is widely used for inducing liver-specific recombination of floxed genes in mice, inducing >90% reduction in the expression of the floxed allele in liver extracts, without evidence of recombination in other tissues including spleen, pancreas, subcutaneous and visceral adipose tissue, heart, muscle, brain, stomach and intestine (Cordoba-Chacon et al. 2015; Sarmento-Cabral et al. 2021; Wolf Greenstein et al. 2017). This knockdown is hepatocyte specific, based on our observations that AAV8-TBGp driven expression of a green florescent protein reporter is isolated to hepatocytes and not expressed in vascular endothelial cells, cholangiocytes, hepatic stellate cells or macrophages (Wolf Greenstein et al. 2017), as well has reports by others showing hepatocyte-specificity of AAV8-TBGp-Cre induced reporter expression (Mu, et al. 2015).

In addition, the previous study (Botusan et al. 2018) presented histological evidence of wound healing at a single time point for 6 mm wounds whereas the present study presented a time course of healing for 8 mm wounds. Thus, the present study may have been better able to capture differences induced by loss of liver IGF-1. Importantly, our findings are consistent with the results of a study on human wounds which found that IGF-1 levels in wound fluid correlated with circulating levels of IGF-1, with the latter having higher concentrations (Wagner et al. 2003). Additionally, human wound IGF-1 levels did not differ between acute wounds created during fasciotomy and chronic wounds caused by infected foreign bodies following repair of tibial fracture despite substantial differences in inflammatory cells and cytokines, suggesting that the local inflammatory environment may not influence IGF-1 levels in human wounds (Wagner et al. 2003). Thus, liver may be a significant source of IGF-1in human wounds as well as mouse wounds.

Much of our knowledge of the role of IGF-1 in wound healing has been generated in studies that increased IGF-1 levels in wounds to improve healing. Local administration of recombinant IGF-1 or adenovirus-mediated overexpression of IGF-1 accelerates wound closure in diabetic mice, ovariectomized mice, and rabbits (Balaji, et al. 2014; Emmerson et al. 2012; Tsuboi, et al. 1995). In addition, keratinocyte specific overexpression of mIGF-1 in mice increased keratinocyte proliferation in wounds and accelerated epithelial closure (Semenova et al. 2008). Effects of IGF-1 on epithelial closure likely arise from the ability of IGF-1 to promote keratinocyte proliferation and migration as demonstrated in cell culture studies using both cell lines and primary cells derived from rodent and humans (Emmerson et al. 2012; Haase et al. 2003; Semenova et al. 2008). Results of these studies are consistent with our findings that reductions in wound IGF-1 levels by ablation of liver IGF-1 results in delayed epithelial closure of skin wounds.

Elevation of IGF-1 in wounds also can enhance dermal healing. Topical application of IGF-1 along with IGFBP1, or adenoviral-mediated overexpression of IGF-1, increased granulation tissue formation in excisional wounds of diabetic mice (Balaji et al. 2014; Tsuboi et al. 1995) and increased collagen deposition and breaking strength of incisional wounds in rats (Jyung, et al. 1994). Effects of IGF-1 on granulation tissue are likely mediated in part by the ability of IGF-1 to promote proliferation, migration, survival and contraction of cultured fibroblasts from various sources (Brandt et al. 2015; Kanekar et al. 2000). Additionally, topical application of IGF-1 with IGFBP1, or adenoviral-mediated overexpression of IGF-1, can promote angiogenesis in wounds of diabetic mice (Balaji et al. 2014; Tsuboi et al. 1995). Effects of IGF-1 on angiogenesis is likely due in part to the ability of IGF-1 to stimulate endothelial cell migration and tube formation as demonstrated in vitro using both cell lines and primary cells (Deng et al. 2012; Nakao-Hayashi et al. 1992). Results of these studies are consistent with our findings that reduction of wound IGF-1 levels by ablation of liver IGF-1 results in reduced angiogenesis and granulation tissue formation in skin wounds.

Perhaps less well studied are anti-inflammatory effects of IGF-1 during wound healing. Locally administered IGF-1 reduced macrophage and neutrophil accumulation in wounds of ovariectomized mice (Emmerson et al. 2012), suggesting such an anti-inflammatory role. Consistent with this idea, keratinocyte-specific overexpression of IGF-1 in mouse skin suppressed allergic contact dermatitis associated with increased Foxp3+ Treg cells (Johannesson, et al. 2014). In addition, increasing IGF-1 levels reduced macrophage accumulation in sciatic nerve in a mouse model of amyotrophic lateral sclerosis (Ji, et al. 2018), and decreased macrophage infiltration into atherosclerotic lesions in mice (Sukhanov, et al. 2007). Results of these studies are consistent with our findings that reduction of wound IGF-1 levels by ablation of liver IGF-1 results in persistent macrophage accumulation in skin wounds. The increased macrophage accumulation in the present study is associated with reduced angiogenesis and granulation tissue formation, which appears to contrast with previous studies showing that macrophages promote these processes (Goren, et al. 2009; Lucas, et al. 2010; Mirza, et al. 2009). However, we speculate that the persistent macrophage accumulation induced by liver IGF-1 knockdown may be associated with a dysregulated phenotype that does not promote healing. We plan on testing this idea in future studies.

Ablation of liver IGF-1 and consequent reduction of wound IGF-1 levels resulted in what may be considered as modest, but significant, impairments in epithelial closure, angiogenesis and granulation tissue formation. The modest impairments may not be surprising as wound IGF-1 levels were not completely ablated and a variety of other growth factors and cytokines are known to promote wound cell function (Werner and Grose 2003). Previous studies have demonstrated that local wound cells express IGF-1, including keratinocytes, fibroblasts and macrophages (Brown et al. 1997; Gartner et al. 1992; Todorovic et al. 2008). These cells likely produce the ~40% of wound IGF-1 levels that remained after ablation of liver IGF-1 and likely promote the function of other wound cells. Further study is needed using cell-type specific targeting to determine the impact of IGF-1 production by these cells on wound healing. In addition, although we did not observe a change in blood glucose levels after liver IGF-1 knockdown, a preliminary study in our laboratory indicated increased insulin (0.7 ± 0.6 ng/ml for AAV-null mice versus 1.8 ± 0.9 ng/ml for AAV-cre mice; n = 12 each group) and growth hormone levels (2.7 ± 4.3 ng/ml

for AAV-null mice versus 21.8 ± 16.1 ng/ml for AAV-cre mice; n = 12 each group) on day 7 post-liver IGF-1 knockdown. Thus, we cannot rule out potential effects of acute increases in insulin and growth hormone on wound healing; however, both are anabolic and might be expected to improve healing and not impede healing.

In conclusion, our data demonstrate that ablation of liver IGF-1 in adult mice leads to ~60% decrease in skin wound IGF-1 levels resulting in delayed wound re-epithelialization, impaired granulation tissue formation and angiogenesis along with persistent macrophage accumulation. Thus, liver is a primary source of IGF-1 in skin wounds, which may also have implications for wound healing outcomes in individuals with metabolic disease, which is known to impair both liver function and wound healing.

Supplementary Material

Refer to Web version on PubMed Central for supplementary material.

Acknowledgements

All authors thank Dr. Luisa A. DiPietro and Dr. Giamila Fantuzzi for their input on aspects of presentation of this manuscript.

Funding:

This study was supported by VA grant I01RX002636 to RDK and TJK and NIGMS grant R35GM136228 to TJK.

Data availability

No large datasets were generated in this study. Primary research data will be made available upon request to the corresponding author.

References

Balaji S, LeSaint M, Bhattacharya SS, Moles C, Dhamija Y, Kidd M, Le LD, King A, Shaaban A, Crombleholme TM, et al. 2014 Adenoviral-mediated gene transfer of insulin-like growth factor 1 enhances wound healing and induces angiogenesis. J Surg Res 190 367–377. [PubMed: 24725678]

Blakytny R & Jude E 2006 The molecular biology of chronic wounds and delayed healing in diabetes. Diabet Med 23 594–608. [PubMed: 16759300]

Botusan IR, Zheng X, Narayanan S, Grunler J, Sunkari VG, Calissendorff FS, Ansurudeen I, Illies C, Svensson J, Jansson JO, et al. 2018 Deficiency of liver-derived insulin-like growth factor-I (IGF-I) does not interfere with the skin wound healing rate. PLoS One 13 e0193084. [PubMed: 29534073]

Brandt K, Grunler J, Brismar K & Wang J 2015 Effects of IGFBP-1 and IGFBP-2 and their fragments on migration and IGF-induced proliferation of human dermal fibroblasts. Growth Horm IGF Res 25 34–40. [PubMed: 25468444]

Brown DL, Kane CD, Chernausek SD & Greenhalgh DG 1997 Differential expression and localization of insulin-like growth factors I and II in cutaneous wounds of diabetic and nondiabetic mice. Am J Pathol 151 715–724. [PubMed: 9284820]

Cordoba-Chacon J, Majumdar N, List EO, Diaz-Ruiz A, Frank SJ, Manzano A, Bartrons R, Puchowicz M, Kopchick JJ & Kineman RD 2015 Growth Hormone Inhibits Hepatic De Novo Lipogenesis in Adult Mice. Diabetes 64 3093–3103. [PubMed: 26015548]

Deng M, Wang Y, Zhang B, Liu P, Xiao H & Zhao J 2012 New proangiogenic activity on vascular endothelial cells for C-terminal mechano growth factor. Acta Biochim Biophys Sin (Shanghai) 44 316–322. [PubMed: 22382131]

Eming SA, Martin P & Tomic-Canic M 2014 Wound repair and regeneration: mechanisms, signaling, and translation. Sci Transl Med 6 265sr266.

Emmerson E, Campbell L, Davies FC, Ross NL, Ashcroft GS, Krust A, Chambon P & Hardman MJ 2012 Insulin-like growth factor-1 promotes wound healing in estrogen-deprived mice: new insights into cutaneous IGF-1R/ERalpha cross talk. J Invest Dermatol 132 2838–2848. [PubMed: 22810305]

Gartner MH, Benson JD & Caldwell MD 1992 Insulin-like growth factors I and II expression in the healing wound. J Surg Res 52 389–394. [PubMed: 1350650]

Goren I, Allmann N, Yogev N, Schurmann C, Linke A, Holdener M, Waisman A, Pfeilschifter J & Frank S 2009 A transgenic mouse model of inducible macrophage depletion: effects of diphtheria toxin-driven lysozyme M-specific cell lineage ablation on wound inflammatory, angiogenic, and contractive processes. Am J Pathol 175 132–147. [PubMed: 19528348]

Haase I, Evans R, Pofahl R & Watt FM 2003 Regulation of keratinocyte shape, migration and wound epithelialization by IGF-1- and EGF-dependent signalling pathways. J Cell Sci 116 3227–3238. [PubMed: 12829742]

Ji Y, Duan W, Liu Y, Liu Y, Liu C, Li Y, Wen D, Li Z & Li C 2018 IGF1 affects macrophage invasion and activation and TNF-alpha production in the sciatic nerves of female SOD1G93A mice. Neurosci Lett 668 1–6. [PubMed: 29294332]

Johannesson B, Sattler S, Semenova E, Pastore S, Kennedy-Lydon TM, Sampson RD, Schneider MD, Rosenthal N & Bilbao D 2014 Insulin-like growth factor-1 induces regulatory T cell-mediated suppression of allergic contact dermatitis in mice. Dis Model Mech 7 977–985. [PubMed: 25056699]

Jyung RW, Mustoe JA, Busby WH & Clemmons DR 1994 Increased wound-breaking strength induced by insulin-like growth factor I in combination with insulin-like growth factor binding protein-1. Surgery 115 233–239. [PubMed: 7508640]

Kanekar S, Borg TK, Terracio L & Carver W 2000 Modulation of heart fibroblast migration and collagen gel contraction by IGF-I. Cell Adhes Commun 7 513–523. [PubMed: 11051461]

Koh TJ & DiPietro LA 2011 Inflammation and wound healing: the role of the macrophage. Expert Rev Mol Med 13 e23. [PubMed: 21740602]

Lucas T, Waisman A, Ranjan R, Roes J, Krieg T, Muller W, Roers A & Eming SA 2010 Differential roles of macrophages in diverse phases of skin repair. J Immunol 184 3964–3977. [PubMed: 20176743]

Martins-Green M, Petreaca M & Wang L 2013 Chemokines and Their Receptors Are Key Players in the Orchestra That Regulates Wound Healing. Adv Wound Care (New Rochelle) 2 327–347. [PubMed: 24587971]

Mirza R, DiPietro LA & Koh TJ 2009 Selective and specific macrophage ablation is detrimental to wound healing in mice. Am J Pathol 175 2454–2462. [PubMed: 19850888]

Mirza RE & Koh TJ 2015 Contributions of cell subsets to cytokine production during normal and impaired wound healing. Cytokine 71 409–412. [PubMed: 25281359]

Mirza RE, Fang MM, Ennis WJ & Koh TJ 2013 Blocking interleukin-1beta induces a healing-associated wound macrophage phenotype and improves healing in type 2 diabetes. Diabetes 62 2579–2587. [PubMed: 23493576]

Mirza RE, Fang MM, Weinheimer-Haus EM, Ennis WJ & Koh TJ 2014 Sustained inflammasome activity in macrophages impairs wound healing in type 2 diabetic humans and mice. Diabetes 63 1103–1114. [PubMed: 24194505]

Mu X, Espanol-Suner R, Mederacke I, Affo S, Manco R, Sempoux C, Lemaigre FP, Adili A, Yuan D, Weber A, et al. 2015 Hepatocellular carcinoma originates from hepatocytes and not from the progenitor/biliary compartment. J Clin Invest 125 3891–3903. [PubMed: 26348897]

Nakao-Hayashi J, Ito H, Kanayasu T, Morita I & Murota S 1992 Stimulatory effects of insulin and insulin-like growth factor I on migration and tube formation by vascular endothelial cells. Atherosclerosis 92 141–149. [PubMed: 1378740]

Sarmento-Cabral A, Del Rio-Moreno M, Vazquez-Borrego MC, Mahmood M, Gutierrez-Casado E, Pelke N, Guzman G, Subbaiah PV, Cordoba-Chacon J, Yakar S, et al. 2021 GH directly inhibits steatosis and liver injury in a sex-dependent and IGF1-independent manner. J Endocrinol 248 31–44. [PubMed: 33112796]

Semenova E, Koegel H, Hasse S, Klatte JE, Slonimsky E, Bilbao D, Paus R, Werner S & Rosenthal N 2008 Overexpression of mIGF-1 in keratinocytes improves wound healing and accelerates hair follicle formation and cycling in mice. Am J Pathol 173 1295–1310. [PubMed: 18832567]

Singer AJ & Clark RA 1999 Cutaneous wound healing. N Engl J Med 341 738–746. [PubMed: 10471461]

Sukhanov S, Higashi Y, Shai SY, Vaughn C, Mohler J, Li Y, Song YH, Titterington J & Delafontaine P 2007 IGF-1 reduces inflammatory responses, suppresses oxidative stress, and decreases atherosclerosis progression in ApoE-deficient mice. Arterioscler Thromb Vasc Biol 27 2684–2690. [PubMed: 17916769]

Todorovic V, Pesko P, Micev M, Bjelovic M, Budec M, Micic M, Brasanac D & Ilic-Stojanovic O 2008 Insulin-like growth factor-I in wound healing of rat skin. Regul Pept 150 7–13. [PubMed: 18597865]

Tsuboi R, Shi CM, Sato C, Cox GN & Ogawa H 1995 Co-administration of insulin-like growth factor (IGF)-I and IGF-binding protein-1 stimulates wound healing in animal models. J Invest Dermatol 104 199–203. [PubMed: 7530269]

Vandesompele J, De Preter K, Pattyn F, Poppe B, Van Roy N, De Paepe A & Speleman F 2002 Accurate normalization of real-time quantitative RT-PCR data by geometric averaging of multiple internal control genes. Genome Biol 3 RESEARCH0034.

Wagner S, Coerper S, Fricke J, Hunt TK, Hussain Z, Elmlinger MW, Mueller JE & Becker HD 2003 Comparison of inflammatory and systemic sources of growth factors in acute and chronic human wounds. Wound Repair Regen 11 253–260. [PubMed: 12846912]

Werner S & Grose R 2003 Regulation of wound healing by growth factors and cytokines. Physiol Rev 83 835–870. [PubMed: 12843410]

Wolf Greenstein A, Majumdar N, Yang P, Subbaiah PV, Kineman RD & Cordoba-Chacon J 2017 Hepatocyte-specific, PPARgamma-regulated mechanisms to promote steatosis in adult mice. J Endocrinol 232 107–121. [PubMed: 27799461]

Yakar S, Liu JL, Stannard B, Butler A, Accili D, Sauer B & LeRoith D 1999 Normal growth and development in the absence of hepatic insulin-like growth factor I. Proc Natl Acad Sci U S A 96 7324–7329. [PubMed: 10377413]

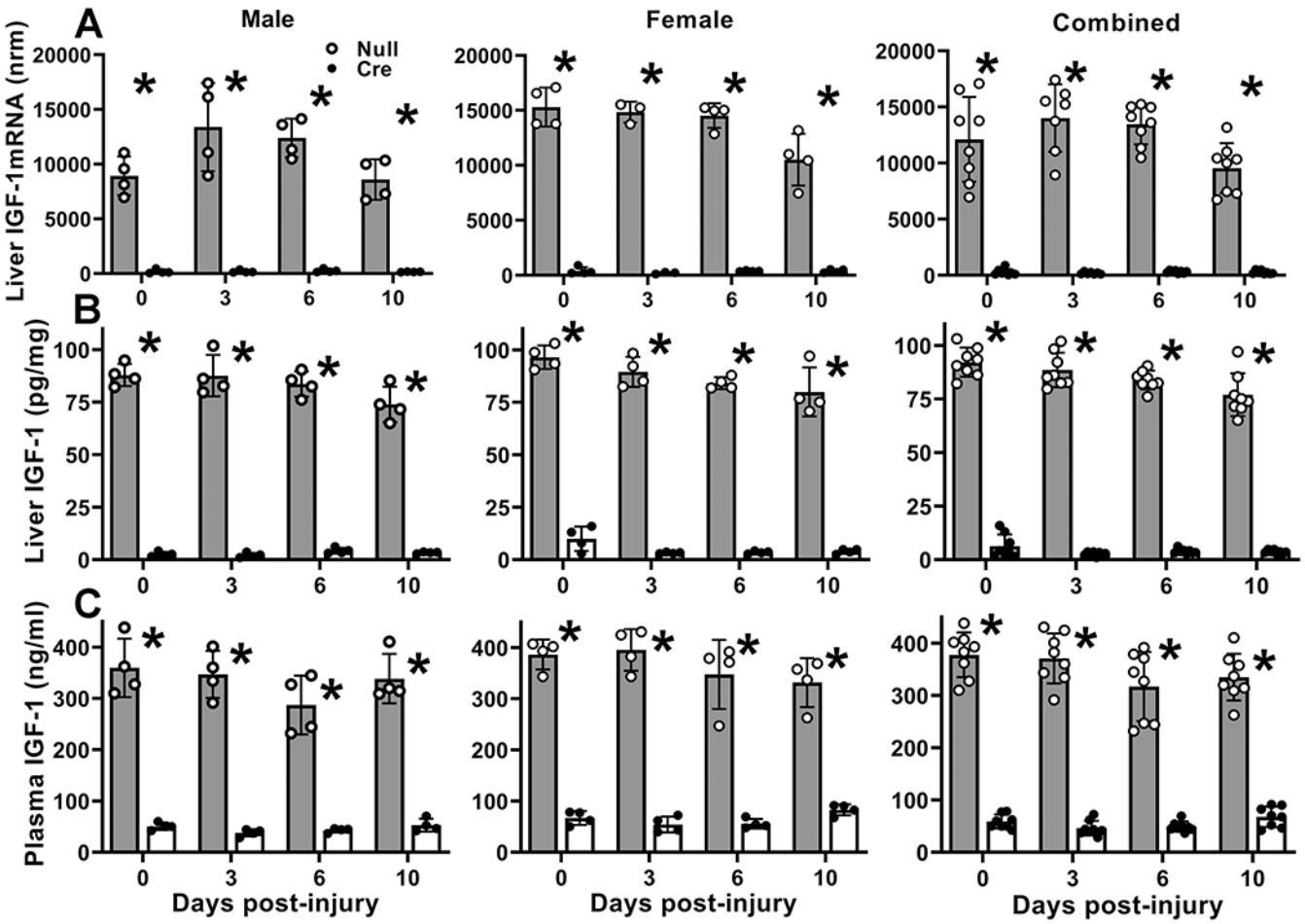

Figure 1. Liver IGF-1 knockdown reduced blood plasma IGF-1 levels.

Liver-specific knockdown of IGF-1 induced by administering AAV8.TBGp.Cre (AAV-Cre) to adult IGF-1 fl/fl mice; controls injected with empty AAV8.pTBG.Null (AAV-Null). (**A**) Liver IGF-1 mRNA levels assessed by real time PCR. IGF-1 mRNA copy numbers normalized (nrm) to those of GAPDH and RPL4 housekeeping genes. (**B**) Liver IGF-1 protein levels assessed by ELISA. (**C**) Blood plasma IGF-1 protein levels assessed by ELISA. For each data set, two-way ANOVA showed significant main effect of IGF-1 knockdown and significant interaction between IGF-1 knockdown and time point. *****mean value for AAV-Cre significantly different from that for AAV-Null at same time point by Sidak's multiple comparisons test; $P < 0.05$. Data presented as mean ± SD, n = 4 male and 4 female mice per assay.

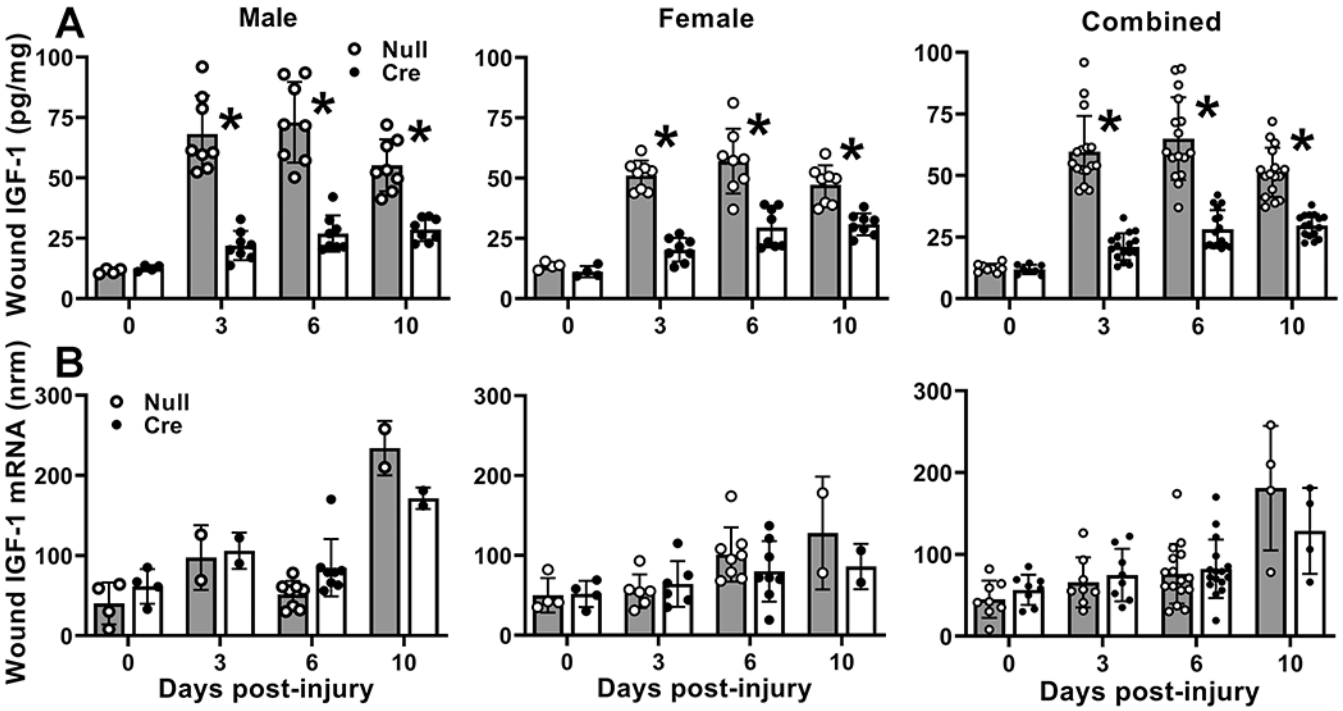

Figure 2. Liver IGF-1 knockdown reduced skin wound IGF-1 protein but not mRNA levels.

Liver-specific knockdown of IGF-1 induced by administering AAV8.TBGp.Cre (AAV-Cre) to adult IGF-1 fl/fl mice; controls injected with empty AAV8.pTBG.Null (AAV-Null). (**A**) Wound IGF-1 protein levels assessed by ELISA. Two-way ANOVA showed significant main effects of IGF-1 knockdown and time point as well as significant interaction between IGF-1 knockdown and time point. *****mean value for AAV-Cre significantly different from that for AAV-Null at same time point by Sidak's multiple comparisons test; $P < 0.05$. (**B**) Wound IGF-1 mRNA levels assessed by real time PCR. IGF-1 mRNA copy numbers normalized (nrm) to those of GAPDH and RPL4 housekeeping genes. Two-way ANOVA showed significant main effect of time point but not of liver IGF-1 knockdown. Data presented as mean ± SD. For protein data, normal dorsal skin or n = 2 wounds from each 4 male and 4 female mice on D0, D3, D6 and D10. For mRNA data, normal dorsal skin or n = 2 wounds from each of 4 male and 4 female mice on D0 and D6, and 3 female mice on D3; n = 1 wound for each of 2 mice on D3 for male mice and D10 for both male and female mice.

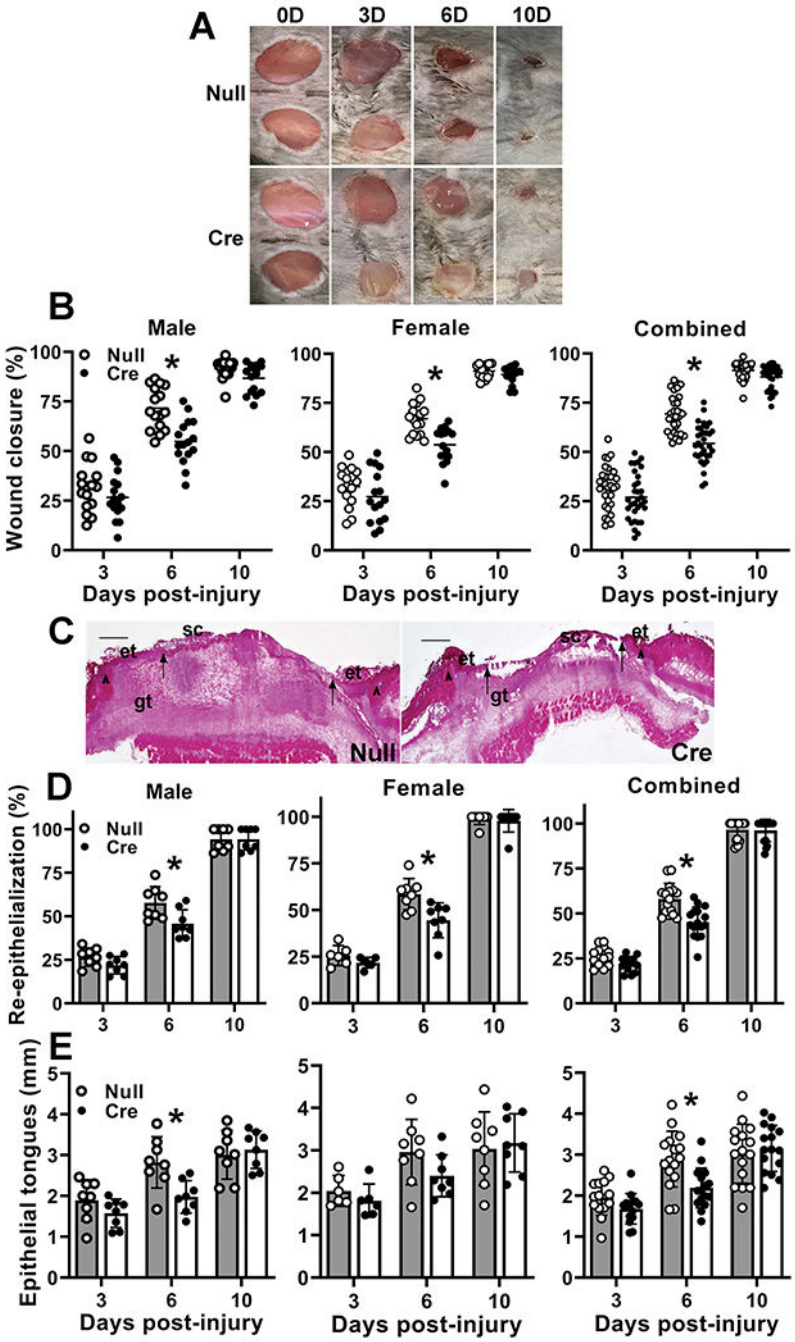

Figure 3. Liver IGF-1 knockdown delayed re-epithelialization.

Liver-specific knockdown of IGF-1 induced by administering AAV8.TBGp.Cre (AAV-Cre) to adult IGF-1 fl/fl mice; controls injected with empty AAV8.pTBG.Null (AAV-Null). (A) Representative images of external surface of D6 wounds from AAV-Null and AAV-Cre treated mice. (B) Wound closure assessed in digital images of wound surface, expressed as % closure from original wound area. (C) Representative images of hematoxylin and eosin stained cryosections of center of D6 wounds from AAV-Null and AAV-Cre treated mice. ep: epithelium, gt: granulation tissue, sc: scab. Arrowheads indicate wound edges and

arrows indicate tips of epithelial tongues migrating into wound. Scale bar = 0.5 mm. (D) Re-epithelialization assessed in cryosections of wound center depicted in (C), expressed as % closure from wound edges in section. (E) Length of epithelial tongues measured in cryosections of wound center depicted in (C), measured as distance between wound edge to end of epithelial tongue, summed across the two sides of the wound. For each data set, two-way ANOVA showed significant main effects of IGF-1 knockdown and time point as well as significant interaction between IGF-1 knockdown and time point. *****mean values significantly different between AAV-Cre and AAV-Null treated mice at same time point by Sidak's multiple comparisons test; $P < 0.05$. Data presented as mean ± SD, n = 2 wounds from each of 4 male and 4 female mice per assay.

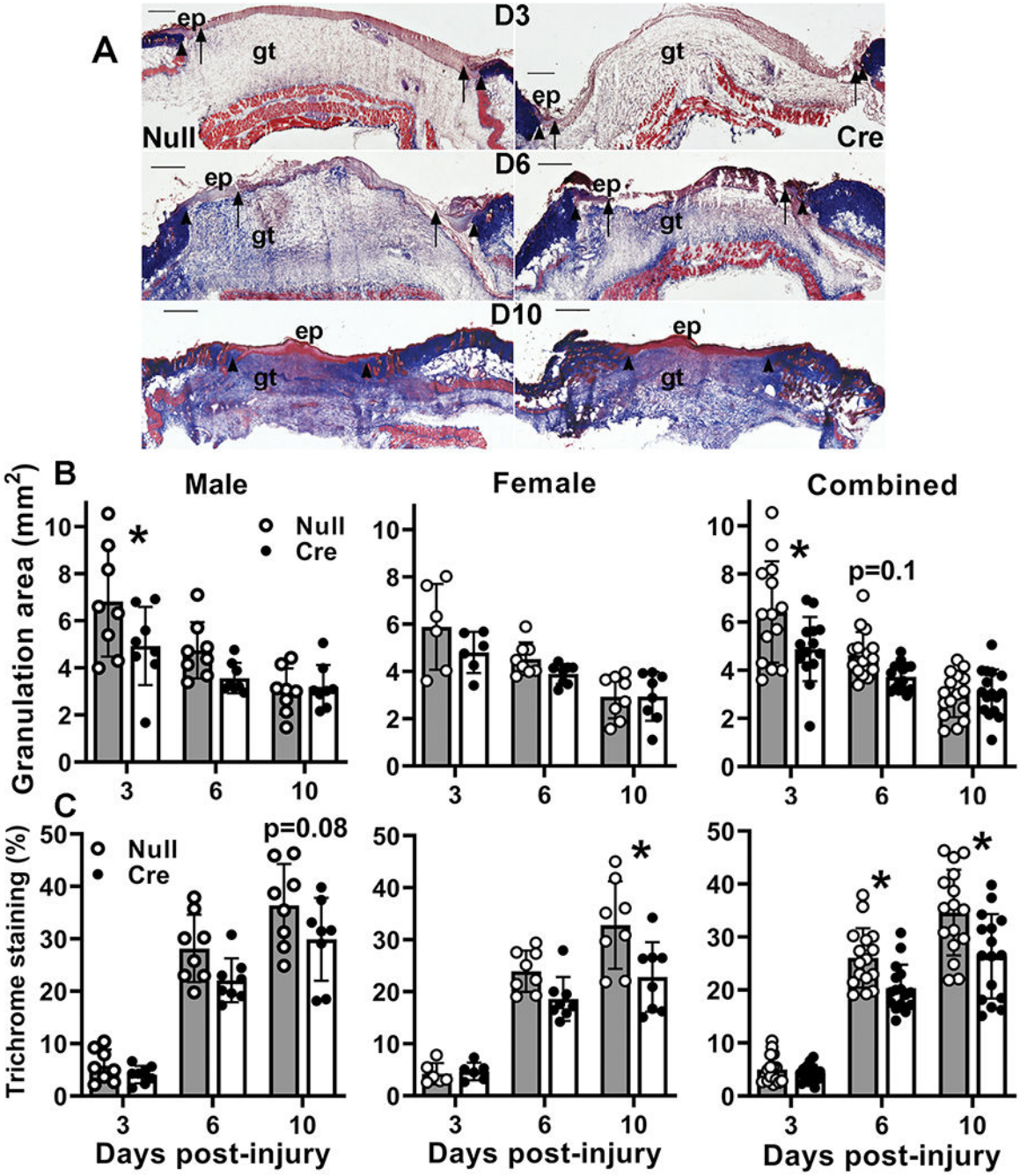

Figure 4. Liver IGF-1 knockdown impaired skin wound granulation tissue formation and maturation.

Liver-specific knockdown of IGF-1 induced by administering AAV8.TBGp.Cre (AAV-Cre) to adult IGF-1 fl/fl mice; controls injected with empty AAV8.pTBG.Null (AAV-Null). (A) Representative images of Trichrome stained cryosections of center of day 6 wounds from AAV-Null and AAV-Cre treated mice. ep: epithelium, gt: granulation tissue. Arrows indicate tips of epithelial tongues migrating into wound. Scale bar = 0.5 mm. (B) Granulation tissue area assessed in cryosections of wound center depicted in (A). (C) Collagen deposition assessed in Trichrome stained cryosections of wound center depicted in (A), expressed

as % area stained blue. For each data set, two-way ANOVA showed significant main effects of IGF-1 knockdown and time point as well as significant interaction between IGF-1 knockdown and time point. *****mean values significantly different between AAV-Cre and AAV-Null treated mice at same time point by Sidak's multiple comparisons test; $P < 0.05$. Data presented as mean ± SD, n = 2 wounds from each of 4 male and 4 female mice per assay.

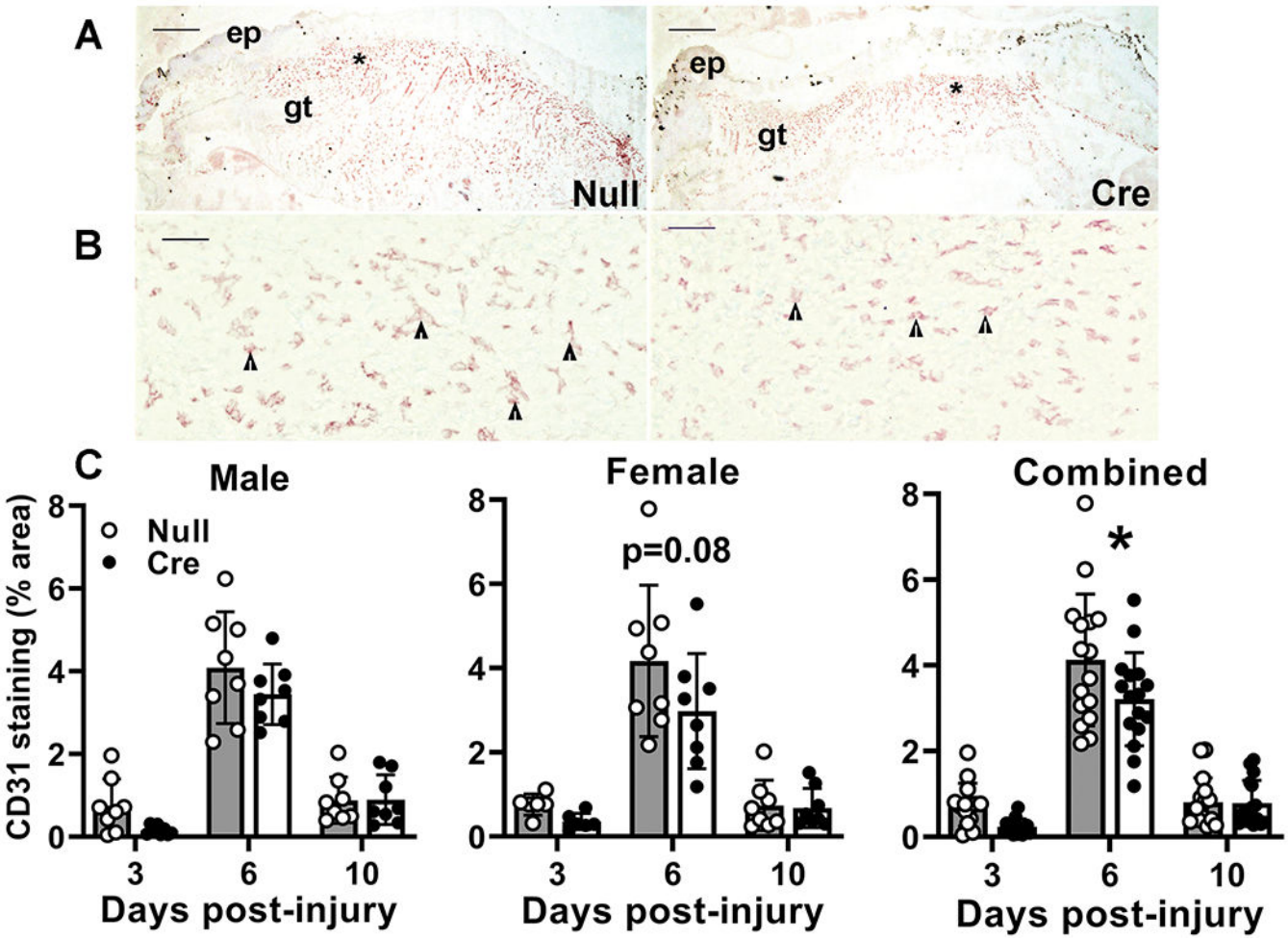

Figure 5. Liver IGF-1 knockdown impaired skin wound angiogenesis.

Liver-specific knockdown of IGF-1 induced by administering AAV8.TBGp.Cre (AAV-Cre) to adult IGF-1 fl/fl mice; controls injected with empty AAV8.pTBG.Null (AAV-Null). Controls injected with empty AAV8 (AAV-Null). (A and B) Low and high magnification images of CD31 stained cryosections of center of day 6 wounds from AAV-Null and AAV-Cre treated mice. ep: epithelium, gt: granulation tissue. Asterisks in (A) indicate area of wound depicted at higher magnification in (B). Arrowheads in (B) indicate positively stained endothelial cells. Scale bar for A = 0.5 mm, for B = 50 μm. (C) Angiogenesis assessed in cryosections of wound center depicted in (A) expressed as % area stained for CD31. Two-way ANOVA showed significant main effects of IGF-1 knockdown and time point. *****mean values significantly different between AAV-Cre and AAV-Null treated mice at same time point by Sidak's multiple comparisons test; $P < 0.05$. Data presented as mean ± SD, n = 2 wounds from each of 4 male and 4 female mice per assay.

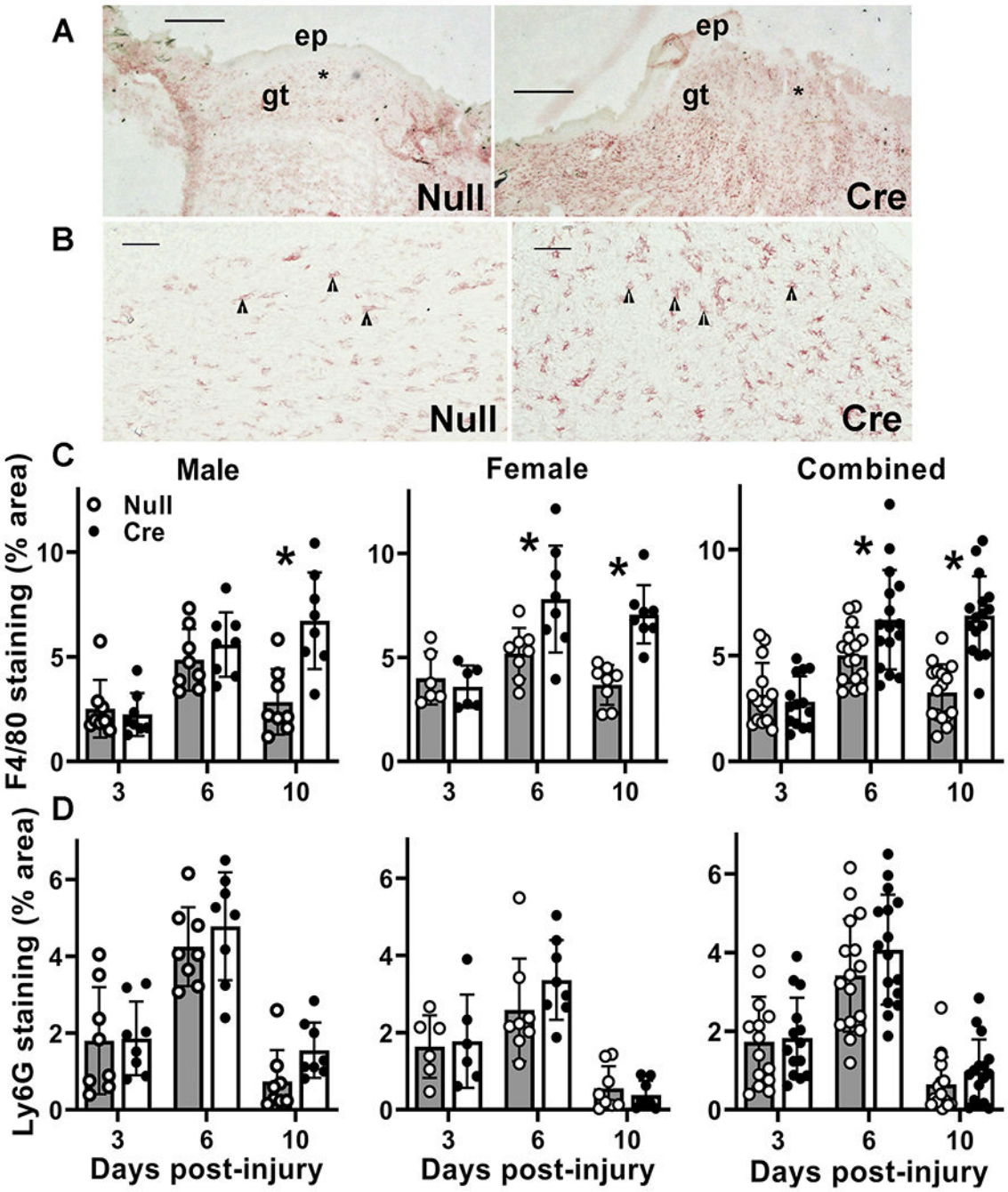

Figure 6. Liver IGF-1 knockdown results in persistent skin wound macrophage accumulation.

Liver-specific knockdown of IGF-1 induced by administering AAV8.TBGp.Cre (AAV-Cre) to adult IGF-1 fl/fl mice; controls injected with empty AAV8.pTBG.Null (AAV-Null). (A and B) Low and high magnification images of F4/80 stained cryosections from center of day 10 wounds from AAV-Null and AAV-Cre treated mice. ep: epithelium, gt: granulation tissue. Asterisks in (A) indicate area of wound depicted at higher magnification in (B). Arrowheads in (B) indicate positively stained macrophages. Scale bar for A = 0.5 mm, for B = 50 μm. (C) Macrophage accumulation assessed in cryosections of wound center depicted in (A

and B), expressed as % area stained for F4/80. Two-way ANOVA showed significant main effects of IGF-1 knockdown and time point as well as significant interaction between IGF-1 knockdown and time point. *****mean value for AAV-Cre significantly different from that for AAV-Null at same time point by Sidak's multiple comparisons test; $P < 0.05$. (D) Neutrophil accumulation assessed in cryosections of wound center expressed as % area stained for Ly6G. [#]Two-way ANOVA showed significant main effect of time point. Data presented as mean ± SD, n = 2 wounds from each of 4 male and 4 female mice per assay.